Research Square

Preprints are preliminary reports that have not undergone peer review.
They should not be considered conclusive, used to inform clinical practice,
or referenced by the media as validated information.

Effect of Graphene Oxide(GO) Nanoscales on the Structural and Optical Properties of TiO_2/PVP Thin Films Prepared by the Sol–Gel Method

Othman S. Bander
University of Anbar
Mahir N. Thameel
esp.mahern.thumail@uoanbar.edu.iq

University of Anbar

Research Article

Keywords: TiO2 thin films, PVP, graphene oxide, reduced graphene oxide, sol–gel method, optical band gap, FESEM, AFM, FTIR and UV–Vis spectroscopy

Posted Date: May 21st, 2026

DOI: https://doi.org/10.21203/rs.3.rs-9621255/v1

License: This work is licensed under a Creative Commons Attribution 4.0 International License.
Read Full License

Additional Declarations: No competing interests reported.

Abstract

Hybrid TiO_2/PVP thin films containing graphene oxide (GO) nanostructures were prepared by a sol–gel spin-coating technique and were examined to determine the impact of GO doping on the structural and optical characteristics of the films. Structural studies by XRD show the emergence of a largely nanocrystalline or semi-amorphous TiO_2 phase embedded within the polymer matrix, accompanied by increasing structural disorder and lattice expansion with increasing GO content. Structural characterization (FESEM and AFM) reveals nanoscale grain formation and a gradual evolution in film morphology, reflecting graphene-induced changes in film formation mechanisms. Optical analyses reveal strong absorption in the ultraviolet but high transmittance (above 80%) in the visible range. The optical band gap of the film decreases from 3.8 eV to 3.5 eV as the GO content increases, due to the introduction of localised electronic states, increased interaction between interfaces, and band tailing effects. FTIR measurements reveal the formation of interfacial bonds between TiO_2, PVP and graphene oxide, indicating the creation of a hybrid organic-inorganic structure. These findings show that graphene oxide is an efficient band-gap modifier and microstructural controller for TiO_2/PVP hybrids. The work offers insights into the fundamental mechanisms of optical transitions and disorder in nanostructured hybrid thin films, which are potential candidates for optoelectronic and photocatalytic devices.

1. Introduction

Titanium dioxide (TiO_2) is one of the most commonly investigated oxide semiconductors because of its low cost, thermal stability, environmental compatibility and various optical properties[1]. It's widely used in creating photocatalysts, self-cleaning materials, and various optical devices, including dielectrics, gas sensors, and photo-electrochemical devices[2]. However, one major limitation of TiO_2 is its large band gap, which means it absorbs light mostly in the ultraviolet region, limiting its use in the visible spectrum [3]. Despite this, TiO_2 has proven to be an excellent ultraviolet filter material for many optical applications, because of its superior optical properties, chemical inertness, and relatively low cost[4, 5]. In particular, nanocomposites made from TiO_2 have some remarkable properties, such as a high refractive index and strong UV absorption capacity, making them perfect for applications that require good light scattering and protection from harmful UV radiation[6]. As a result, TiO_2 is commonly used in sunscreens and protective coatings, as well as in optical devices like solar cells and antireflective layers[7].

The problem with TiO_2 is that it's really brittle, which makes it hard to work with. This challenge could be solved by combining it with organic and inorganic materials to create a hybrid system [9]. Polyvinylpyrrolidone (PVP) is one of the ideal polymers for such hybrid systems, because it is soluble in polar solvents - hence ensuring good viscosity control in spin coating technique during the formation of the thin film, stably preserves the final thin-film except for few annealing steps and can act as a structure-directing agent throughout sol-gel process conditions afterwards [9–12]. The hybrid-composite

TiO_2-PVP thin-films have been found to be smooth and have a good miscibility of the polymer with the TiO_2 network, which suggests that it can be used for further modification in this TiO_2/PVP system.[13]

Also, a common approach is to embed graphene/graphene oxide (GO) nanostructures into TiO_2 based system [14]. The graphene-based additive has a large surface area, can conduct charges and can help to passivate the defects that will be affecting the absorptive potential characteristics and the optical band gap of the TiO_2 composites (isoelectronic midpoint).[15]

So, it is conceivable to assume that perhaps a combination of TiO_2, PVP and graphene nanomaterials can be embedded in a thin film structure. PVP matrix helps to the distribution, TiO_2 provides the semiconducting oxide backbone and GO introduces local electronic/project structural effects of GO[14]. The addition of GO provides different band gap energy (depending on the degree of oxidation) and the formation of Ti-O-C bonds enhances visible light photocatalytic activity [16]. This multifunctionality is translated to new functional materials with enhanced catalytic/optical/electronic properties that can be used for novel efficient coating and energy conversion systems. The presence of high surface area, and electro-chemical and mechanical stability of GO also optoelectronic potential and high photocatalytic performance and stability of TiO_2 could be harnessed to achieve multifunctional thin films[17].

In the current work it's been focus on fabricating thin films of TiO_2/PVP/GO as a UV filter and also study the effect of GO on film properties. The addition of GO to the TiO_2 (as in this study) is one of the ways to narrow TiO_2 band gap thereby increasing the photocatalytic activity. Band gap narrowing will enhance the light absorption (particularly in the visible to near-infrared region), which helps not only the generation of electron-hole pairs but also provide a high driving force for charge separation. Which will be proved in our next project.

2. Experimental Background and Characterization Strategy

TiO_2/PVP hybrid thin films containing graphene oxide nanostructures were studied using a sol–gel method. Hydrolysis and condensation of Titanium Isopropoxide (TTIP) precursor were carry out using an alcoholic medium under controlled acidity condition whereby 1 ml of (TTIP) was mixed with 10 ml of Isopropanol and stirred for 5 min followed by drop wise addition of 1 ml Acetic acid (added slow to avoid the aggregation mass media precursor solution) 0.1 ml of Isopropanol diluted with 0.2 ml distilled water and then dripped in the mixture then allowed to stir at room temperature for a period of 60 min. and then sits overnight for the purpose of aging. 0.1 g of PVP was dissolved in 10 ml Isopropanol and stirred for 30 min to make sure a complete dissolving. Both mixtures were then mixed together (1:1) to get a group of hybrid sol-gel with same phase and appropriate viscosity for film deposition. Low loading levels of 1mg/ml GO are accurately placed in Isopropanol and dispersed in the solvent by sonication to reduce agglomeration. Different solutions of TiO_2/PVP/GO with various GO have been prepared (0.1, 0.25, 0.5, 0.75 and 1%) and spin coated on well cleaned glass and Quartz substrates at 3000 rpm for 1 min gives rough thickness of about 1µm. Then several treatments were carried out on the created films, including

drying for 30 min at 40 ^{o}C and a final thermal treatment in an oven at 80 ^{o}C for 10 min to eliminate solvents and endorse the formation of an inorganic network.

Crystallinity and phase development evaluated by XRD. The FESEM image was used to represents the surface morphology and particle distribution while the EDS spectra confirm elemental signature of the deposited material. AFM used to show varied heights and surface textures down to the nanoscale. FTIR employed to identify the chemical bonds and interfacial interactions between TiO_2, PVP and the graphene-based additive. Absorbance and transmittance spectra for the prepared films were determined using UV–Vis spectroscopy. All of these techniques provide a coherent portrait of the performance of graphene doping in the hybrid film.

3. Results and Discussion

3.1 X-ray diffraction analysis

Figure 1 shows the stacked XRD patterns of un-doped TiO_2 and TiO2/PVP films with different concentration of graphene Oxide nanoscales (0.1, 0.25, 0.5, 0.75 and 1% of GO). The wide distribution of intensity in the lower 2θ range, particularly 2θ ≈ 23.5° is overwhelmingly prominent in all the samples with few distinct structural features at higher angles. This behavior is typical for the embedded in situ nanocrystalline oxide domains in amorphous or semi-amorphous polymer matrix and when heat treatment is not enough to develop sharp crystalline peaks[18].the broadening of the diffraction peak may be caused also by very small coherent scattering domains in size (less than 20 nm), high microstrain, or a high amorphous fraction [19]. Coordination of PVP-chains to precursor species stabilizes such intermediate amorphous complexes and modifies the growth mechanism for the oxide network, thus delaying the onset of free-standing crystallite growth in TiO2/PVP films. It typically results in smaller inorganic domains as a result of low temperature processing[20].

Two perspectives will be delivered from incorporation of GO in the films. At a low loading, graphene-based nanosheets may act as heterogeneous nuclei, which help to allow more homogeneous distribution of Ti-species during gel drying and pyrolysis[21]. On the other hand, at higher concentration excess GO nanosheets can introduce local disorder and can reduce the peak intensities by dilution with the amorphous phase, resulting in packing disorder. Also, there is a gradual shift of the diffraction halo towards the smaller diffraction angles, where the d-spacing is gradually increased from 3.78 Å to 3.92 Å (Table 1). In addition, the progressive broadening of the diffraction peak (FWHM increase) at higher concentration of GO shows an increasing of disorder and distortion. This is consistent with the apparent crystallite size which is constantly decreasing from ∼0.9 nm to 0.65 nm. The present diffraction curves are well matched with a situation where the inorganic phase remains in the nanometric scale and well dispersed with a fraction of the polymer phase.

If the samples don't exhibit any feature that is associated with highly crystalline anatase or rutile films (sharp and intense peaks), it is expected that the current structure is accentuated as a low-crystallinity

TiO_2 in a hybrid TiO_2/PVP/GO film. The validity of this consideration is in line with a more sol-gel processed coating, which promotes film continuity and nanometric mixing instead of high temperature ceramic derived TiO_2 crystallization [22].

Table 1
shows the XRD Data for TiO_2/PVP/GO films with different GO loading.

Sample	GO (wt.%)	Main 2θ (deg)	d-spacing (Å)	FWHM (deg)	D (nm)	a (Å)	c (Å)	Structure
TiO_2	0	23.50	3.78	10.5	0.90	3.84*	9.42*	Semi-amorphous
TiO_2/PVP/GO	0.1	23.50	3.78	10.9	0.74	3.84*	9.42*	Semi-amorphous
TiO_2/PVP/GO	0.25	23.50	3.78	11–13	0.60–0.90	3.84*	9.42*	Disordered
TiO_2/PVP/GO	0.5	23.50	3.78	11–12	0.60–0.80	3.84*	9.42*	Poorly crystalline
TiO_2/PVP/GO	0.75	23.09	3.85	11.27	0.72	3.84*	9.42*	Semi-amorphous
TiO_2/PVP/GO	1.0	22.66	3.92	12.57	0.65	3.84*	9.42*	Highly disordered

* Approximated lattice constants based on weak uncertain anatase reflections.

3.2 FESEM morphology and particle-scale structure

Figure 2 presents FESEM images, a heterogeneous nanoscale surface made of grains, nodules and compressed agglomerate-type structures protrude all over the film. Even the size observations in those few cases are clustered to a large extent in the 24–79 nm range that appears to justify the conclusion that constituents or structures with an accurate nanoscale morphology have self-assembled with each other to create an overall coating. Notably, there was no brittle fracturing or hard delamination in the pictures, which meant that continuous films could be formed using the hybrid sol-gel road with PVP.

The general analysis of the microstructures shows that there is no composition with the same surface. Individual bright grains are shaped in one or two, other are larger lumps and others show more concentrated regions of smaller grains. This is not surprising since the introduction of graphene-based additives to a TiO_2/PVP host can change local viscosity, drying stress and packing of inorganic clusters which shapes the entire microstructure .[23]

Optical and interfacial Grains the Grains in the tens-of-nanometers order are also useful in optical and interfacial applications and smaller Grains can also be used effectively to increase the active adsorption or reaction sites [24]. Nevertheless, even with the nanostructure having a relatively uniform nature, it is

possible to retain visible transparency so long as the size of the feature is reduced to less than the wavelength of visible light to a large enough degree[25]. The multifunctional dual application as optical active coating and high-surface-area nanostructured layer is thereby further justified with the assistance of the micrographs.

3.3 EDS elemental assessment

As shown in Fig. 3, the EDS spectra accompanied with the FESEM results are primarily of expected Ti and O signals strongly demonstrating that oxide phase is deposited. As evidenced by the carbonaceous composition of the hybrid layer, weak additional features could arise from the substrate, residual impurities and/or organic/carbonaceous species that are inherent from their widely used precursors PVP and GO. Due to the high quantitative error of EDS for light elements and the geometry influence on thin-film quantifications (detected volume), it is difficult to quantify the polymer fraction in hybrid thin films.[26]

However, the spectra are wholly consistent with the successful incorporation of TiO_2 into the deposited layers. Interpreted in conjunction with the FESEM images they suggest that not all visible nanoscale features are due to randomly deposited contamination but may be derived from a Ti-containing hybrid thin-film structure.

3.4 AFM topography

Very pronounced nanoscale peaks and valleys can be seen in the AFM images depicted in Fig. 4 that spread over the scanned surface. Table 2 indicates that the surface roughness parameters (Sa, Sq, Ra and Rq) were increased with increasing GO concentration and reach its maximum values at 1% GO. This behavior was ascribed to stacking of GO nanosheets and generate a randomly disperse surface morphology. A mild decline in roughness, corroborating better dispersion and lower agglomeration, is seen at 0.5% GO.

The images demonstrate that graphene doping affects not only the topography of TiO_2/PVP films but by virtue does sharply alter it rather than preserve its original state. Some images show a surface that is comparatively compact and covered with short-range protrusions uniformly scattered; other images reveal the presence of larger undulations and greater topographic contrast.

In other words, the additive alters and restructures as the sol dries, shrinks and becomes solid during film formation. GO sheets, being anisotropic in shape promotes anisotropic packing and the presence of pathways for nanoparticle attachment causing a surface evolution from a smoother polymer appearance to a more rugged nanostructure[27]. It has been shown previously that a modest increase in roughness is beneficial for photocatalysis and sensing as it increases effective surface area[28]. On the contrary, increasing roughness may also lead to more scattering losses and reduced optical transparency[29]. The

surfaces that we observe are either minimal or in a useful nanometric regime, rather than having very rough surfaces.

In both (FESEM) and (AFM) data the resulting nanostructure depends on composition which is consistent with the graphene-based component serving as a microstructural modifier.

Table 2
shows the AFM Data for TiO_2/PVP/GO films with different GO loading.

GO (%)	Sa (nm)	Sq (nm)	Ra (nm)	Rq (nm)	Sy (nm)
0.1%	0.291	0.386	0.253	0.321	6.377
0.25%	0.518	0.777	0.297	0.407	8.783
0.5%	0.651	0.981	0.486	0.574	10.764
0.75%	0.843	1.121	1.230	1.771	19.754
1%	0.966	1.313	1.420	2.064	21.093

3.5 FTIR analysis

FTIR spectra of at least three states (i.e. pure PVP, hybrid film of TiO_2/PVP and TiO_2/PVP film with graphene) are shown in Fig. 5. The broad bands at high frequencies (around 3200–3600 cm^{-1}) arises from the stretching vibration of O-H bonds of water, hydroxyl and other oxygen-containing groups present due to sol-gel process and graphene oxide[30]. The bands in the 2900 cm^{-1} region are from the stretching vibrations of the C-H groups from the polymer backbone[31].

The band at 1650 cm^{-1}, which is usually assigned to stretching of C = O bond of the pyrrolidone ring, is characteristic of PVP[29]. This band can also be shifted and/or have a different intensity in hybrid films than in pure PVP, due to the influence of the metal centers, because the coordination of the metal ions affects the bonding of the carbonyl oxygen atom. Additional PVP bands are found in the fingerprint region (C-N, and ring vibrations)[32].

In the low wavenumbers below 700 cm^{-1} vibrations of Ti – O–Ti bonds are expected. Bands in this region are associated with absorption and enhancement in a network structure of TiO_2[33]. A broadening and shift of the polymer-related and hydroxyl-bands with GO addition may be related to an interaction at the interface rather than a physical mixture[34]. The spectra observed here are in agreement with this: the hybrid film is not a simple mixture, but an organic-inorganic hybrid with chemical interactions, where the functionality derived from graphene is part of the interface.

3.6 UV–Vis absorbance and transmittance

Typical behavior for TiO_2-based thin films, as shown in the optical spectra (Fig. 6), is denoted by strong absorption in ultraviolet region, followed by a rapid drop off in absorbance into the visible range and high increase of transmittance accordingly. Considering that bulk polymer is an insulator and does not have a counteracting semiconductor absorption edge in this same region [35]. Pure PVP has a uniquely different spectral profile than any oxide-containing films.

The incorporation of GO adds in the absorbance of the hybrid films, particularly, in the UV-and near-edge spectral region. There are several mechanisms that may account for this behavior. The broad absorption background is firstly contributed by the graphene-based nanosheets. Second, one can involve interfacial electronic states in lower-energy transitions[36]. Third, the additive may vary the film morphology and/or thickness that modify optical path, and therefore dictating effective absorbance properties [37]. At the same time, the visible transmittance is still relatively high, but the films containing graphene become less transparent than their undoped or less loaded reference (the larger fraction of incident light that is absorbed or scattered).

This trend, from the application perspective, is quite important. For UV-shielding coatings, self-cleaning windows, photodetectors or interfacial layers in optoelectronic devices[38],[39], (i.e. increased absorbance with still appreciable visible transparency) is highly desirable. Thus, the current spectra indicate that doping-in graphene enhances light harvesting while maintaining an operative nontransparency of the films.

3.7 Absorption coefficient and optical band-gap behavior

The absorption-coefficient curves in Fig. 7 are equivalent to the absorbance and demonstrate the strongest optical transitions occur in the ultraviolet region. The Tauc plot also reveals that the hybrid films appear to have an apparent band gap in mid-3 eV whereas the band gap of reference sample is much larger. The labels shown in the Tauc plot (Fig. 7) show that band-gap estimates are similar and seem to be in the range 3.5–3.8 eV for TiO_2-containing hybrid films and 5.3 eV for the polymer-rich PVP reference sample.

The effective optical band gap shrinks compared with the biopolymer with narrowest-gap reference(Table 3). This is usually associated to the formation of the localized energy states in semiconductor-polymer-graphene composites, an enhanced orbital coupling at the interface or oxygen-vacancy induced disorder[40] and defect-induced band tail states[41]. This shifts the absorption edge to longer wavelength[42].

The benefits of band-gap reduction are improved optical response at longer wavelengths. This leads to a better use of near-UV and visible light for photocatalysis and sensing[43]. But for optoelectronic thin films it means that the hybrid film can be compositionally switched from transparent to photoactive[41]. This confirms why current findings continue to suggest that graphene doping is not only a morphological but also band-structure tuning technique for TiO_2/PVP thin films.

Table 3
Approximate optical band-gap trend for TiO_2/PVP/GO films with different GO loading.

Composition class	Approximate Eg trend from supplied figure
PVP-rich reference	Highest apparent gap, about 5.3 eV
Undoped/low-doped TiO_2 hybrid	Near 3.7–3.8 eV
Graphene-containing TiO_2/PVP hybrids	Reduced to roughly 3.5–3.8 eV depending on composition

5. Conclusions

The graphene-based nanostructures-modified TiO_2/PVP thin films are obviously hybrid in nature, in terms of structure, morphology and optical properties. X-ray diffraction shows that TiO_2 (poorly-crystalline or nanocrystalline) is embedded in the polymer matrix.. FESEM shows micron-sized particle-like surface features, which are characteristic of the nanoscale dimension measured by AFM, and examination using AFM indicates how the graphene-derived additive alters the surface topography and feature density. FTIR spectroscopy shows the presence and interaction of TiO_2, PVP and oxygen containing interfacial components. They are strongly UV-absorber with limited optical transparency to the visible spectrum from UV-Vis measurements, and Tauc plots show the decrease in the effective band-gap values for hybrid films with respect to its high-band-gap analog. Observed band gap narrowing and structure disorder effects can be explained in terms of formation of localized states and band tailing due to disorder in hybrid nanostructures.

In conclusion, collectively, we also present evidence to suggest that the light harvesting and electronic structure alterations of sol–gel derivatized TiO_2/PVP films was enhanced by graphene-based doping. The intrinsic features render the system scientifically attractive for photocatalytic, sensing, optoelectronic, and protective-coating applications. Observed band gap narrowing and structure disorder effects can be explained in terms of formation of localized states and band tailing due to disorder in hybrid nanostructures.

Declarations

Funding

This research received no external funding.

Author Contribution

Othman S. Bander supplied the materials and contribute to complete experimental part.Mahir N. Thameel suggested the project and helped with finishing the experimental part also wrote the main

manuscript.All authors reviewed the manuscript,

Acknowledgment

The authors would like to thank the Department of Physics, College of Education for Pure Science, University of Anbar, for the facilities and the constant support during this research work. In particular, the technical staff of Nano Research Center are appreciated for their help in thin film characterization using XRD, FESEM, AFM and UV-Vis.

References

1. L. Coelho, M. Ornelas, B.R. Gomes, B. Moura, The Quest for Sustainable Titanium Dioxide: Conventional and Sustainable Synthesis Approaches and Its Functionalities in Diverse Industries, in *IntechOpen eBooks*, IntechOpen, 2024. 10.5772/intechopen.1007378
2. E. Kumi-Barimah, R. Penhale-Jones, A. Salimian, H.M. Upadhyaya, A. Hasnath, G. Jose, Phase evolution, morphological, optical and electrical properties of femtosecond pulsed laser deposited TiO2 thin films. Sci. Rep. **10**(1) (Jun. 2020). 10.1038/s41598-020-67367-x
3. S.R. Raghavan, TiO2 Nanostructures by Sol-Gel Processing, in *IntechOpen eBooks*, IntechOpen, 2023. 10.5772/intechopen.111440
4. S. Lourduraj, Titanium Dioxide Versatile Solid Crystalline: An Overview, in IntechOpen eBooks, IntechOpen, 2020. 10.5772/intechopen.92056
5. F.B. Emre, Investigation of Physicochemical Properties and Specific Heat Capacity of Tio2 Doped-Polydimethylsiloxane Composites. Nanofabrication. **7** (Sep. 2022). 10.37819/nanofab.007.224
6. M.M. Kobir, S. Tabassum, S. Ahmed, S.I. Sadia, M.A. Alam, Crystallographic Benchmarking on Diffraction Pattern Profiling of Polymorphs-TiO2 by WPPF for Pigment and Acrylic Paint. Archives Curr. Res. Int. **24**(1), 62 (Jan. 2024). 10.9734/acri/2024/v24i1623
7. M. Janus, Application Titanium Dioxide. (2017). 10.5772/intechopen.70121
8. E. Zanchetta, G.D. Giustina, A. Gandin, V. Auzelyte, G. Brusatin, One-step fabrication of high refractive index inorganic nanostructures. J. Solgel Sci. Technol. **107**(1), 122 (Oct. 2021). 10.1007/s10971-021-05633-8
9. W.S. Khan, N.N. Hamadneh, W.A. Khan, Prediction of thermal conductivity of polyvinylpyrrolidone (PVP) electrospun nanocomposite fibers using artificial neural network and prey-predator algorithm, *PLoS ONE*, vol. 12, no. 9, Sep. 2017, 10.1371/journal.pone.0183920
10. Y. Aleeva, B. Pignataro, Recent advances in upscalable wet methods and ink formulations for printed electronics. J. Mater. Chem. C **2**, 6436 (Jan. 2014). 10.1039/c4tc00618f
11. S.A. Hadi, K. Humood, M.A. Jaoudé, H. Abunahla, H.F.A. Shehhi, B. Mohammad, Bipolar Cu/HfO2/p + + Si Memristors by Sol-Gel Spin Coating Method and Their Application to Environmental Sensing, *Scientific Reports*, vol. 9, no. 1, Jul. 2019, 10.1038/s41598-019-46443-x

12. A.E. Danks, S.R. Hall, Z. Schnepp, The evolution of ‘sol–gel’ chemistry as a technique for materials synthesis. Mater. Horiz. **3**(2), 91 (Dec. 2015). 10.1039/c5mh00260e
13. M.-P. Zheng, M. Gu, Y. Jin, G. Jin, Preparation, structure and properties of TiO2–PVP hybrid films. Mater. Sci. Eng., B **77**(1), 55 (Aug. 2000). 10.1016/s0921-5107(00)00465-7
14. R. Wang, K. Shi, D. Huang, J. Zhang, S. An, Synthesis and degradation kinetics of TiO2/GO composites with highly efficient activity for adsorption and photocatalytic degradation of MB. Sci. Rep. **9**(1) (Dec. 2019). 10.1038/s41598-019-54320-w
15. M. Nasr, Elaboration of oxides membranes by electrospinning for photocatalytic applications, *HAL (Le Centre pour la Communication Scientifique Directe)*, Oct. 2017, Accessed: Jul. 2025. [Online]. Available: https://tel.archives-ouvertes.fr/tel-01872723
16. M. Nsar, Elaboration des membranes d’oxydes par electrospinning pour des applications photocatalytiques, *HAL (Le Centre pour la Communication Scientifique Directe)*, Oct. 2017, Accessed: Jan. 2025. [Online]. Available: https://hal.umontpellier.fr/tel-01681200
17. İ.F. Balkaya, Comparison of Graphene Oxide-Titanium Oxide (GO-TiO2) Composite Film Coating Methods on Glass Substrates and Surface Characterization Study, *DergiPark (Istanbul University)*, Aug. 2024, 10.36222/ejt.1536083
18. M. Biesuz et al., First synthesis of silicon nanocrystals in amorphous silicon nitride from a preceramic polymer. Nanotechnology. **30**, 255601 (Mar. 2019). 10.1088/1361-6528/ab0cc8
19. Y. Yao, Improvement of magnetic properties of nanocristalline magnetic soft alloys dedicated to power electronics, *HAL (Le Centre pour la Communication Scientifique Directe)*, Dec. 2015, Accessed: Jan. 2025. [Online]. Available: https://theses.hal.science/tel-01278096
20. N.M. Al-Hada et al., Recent advances in PVP-assisted thermal treatment: Impact on nanostructure properties, potential applications, challenges, and future perspectives. Results Phys. **65**, 107990 (Sep. 2024). 10.1016/j.rinp.2024.107990
21. U. Naknikham, V. Boffa, G. Magnacca, A. Qiao, L.R. Jensen, Y. Yue, Mutual-stabilization in chemically bonded graphene oxide–TiO2 heterostructures synthesized by a sol–gel approach. RSC Adv. **7**(65), 41217 (Jan. 2017). 10.1039/c7ra07472g
22. S. Bai, X. Shen, Graphene–inorganic nanocomposites. RSC Adv. **2**(1), 64 (Nov. 2011). 10.1039/c1ra00260k
23. F. Tardani, W. Néri, C. Zakri, H. Kellay, A. Colin, P. Poulin, Shear Rheology Control of Wrinkles and Patterns in Graphene Oxide Films. Langmuir. **34**(9), 2996 (Feb. 2018). 10.1021/acs.langmuir.7b04281
24. L.I. Abu-Lail, J. Bergendahl, R.W. Thompson, Adsorption of methyl tertiary butyl ether on granular zeolites: Batch and column studies. J. Hazard. Mater. **178**, 363 (Jan. 2010). 10.1016/j.jhazmat.2010.01.088
25. A. Bisht, V. Kumar, P.C. Maity, I. Lahiri, D. Lahiri, Strong and transparent PMMA sheet reinforced with amine functionalized BN nanoflakes for UV-shielding application. Compos. B Eng. **176**, 107274 (Aug. 2019). 10.1016/j.compositesb.2019.107274

26. W. Moon, S.G. Yu, Y.S. Kim, B. Park, W. Jung, H. Song, New strategy to improve the accuracy of quantitative analysis of energy dispersive spectroscopy. Phys. Scr. **99**(3), 35013 (Jan. 2024). 10.1088/1402-4896/ad241e
27. R. Torres–Mendieta, D. Ventura-Espinosa, S. Sabater, J. Láncis, G. Mínguez-Vega, J.A. Mata, In situ decoration of graphene sheets with gold nanoparticles synthetized by pulsed laser ablation in liquids. Sci. Rep. **6**(1) (Jul. 2016). 10.1038/srep30478
28. M. Dehghani, C. David, Light Scattering from Rough Silver Surfaces: Modeling of Absorption Loss Measurements. Nanomaterials. **11**(1), 113 (Jan. 2021). 10.3390/nano11010113
29. A. Ghoshroy, W. Adams, X. Zhang, D.Ö. Güney, Active plasmon injection scheme for subdiffraction imaging with imperfect negative index flat lens. J. Opt. Soc. Am. B **34**(7), 1478 (Jun. 2017). 10.1364/josab.34.001478
30. M.T. Stauffer, *Applications of Molecular Spectroscopy to Current Research in the Chemical and Biological Sciences*. 2016. 10.5772/61896
31. I.A. Safo, M. Werheid, C. Dosche, M. Oezaslan, The role of polyvinylpyrrolidone (PVP) as a capping and structure-directing agent in the formation of Pt nanocubes. Nanoscale Adv. **1**(8), 3095 (Jan. 2019). 10.1039/c9na00186g
32. M. Julinová, L. Vaňharová, D. Šašinková, A. Kalendová, I. Burešová, Characterization and biodegradation of ternary blends of lignosulfonate/synthetic zeolite/polyvinylpyrrolidone for agricultural chemistry. Int. J. Biol. Macromol. **213**, 110 (May 2022). 10.1016/j.ijbiomac.2022.05.153
33. P.K. Singh, S. Mukherjee, C.K. Ghosh, S. Maitra, Spectroscopic Investigation on Sol Gel Derived TiO2 Nanoparticles. J. Adv. Nanomaterials. **2**(3) (Aug. 2017). 10.22606/jan.2017.23004
34. Q. Fu, Z. Yang, H. Jia, Y. Wen, Y. Luo, L. Ding, Integration of experimental methods and molecular dynamics simulations for a comprehensive understanding of enhancement mechanisms in graphene oxide (GO)/rubber composites. J. Polym. Res. **30**(7) (Jun. 2023). 10.1007/s10965-023-03658-x
35. T. Tański, M. Zaborowska, W. Matysiak, POLYVINYLPYRROLIDONE/SILICON DIOXIDE COMPOSITE THIN FILMS – PREPARATION AND ANALYSIS OF PROPERTIES, Arch. Metall. Mater. (Feb. 2018). 10.24425/118930
36. S. Haffad, K.K. Kiprono, Interfacial structure and electronic properties of TiO2/ZnO/TiO2 for photocatalytic and photovoltaic applications: A theoretical study. Surf. Sci. **686**, 10 (Mar. 2019). 10.1016/j.susc.2019.03.006
37. C. Bonavolontà et al., Anomalous evolution of broadband optical absorption reveals dynamic solid state reorganization during eumelanin build-up in thin films. Sci. Rep. **7**(1) (Mar. 2017). 10.1038/s41598-017-00597-8
38. J. Peng et al., Highly transparent, self-cleaning, and UV-shielding composite coating: When eco-friendly waterborne omniphobic surface cooperates with quantum dots. Compos. B Eng. **284**, 111731 (Jul. 2024). 10.1016/j.compositesb.2024.111731

39. T. Shan, X. Hou, X. Yin, X. Guo, Organic photodiodes: device engineering and applications, *Frontiers of Optoelectronics*, vol. 15, no. 1. Higher Education Press, Dec. 01, 2022. 10.1007/s12200-022-00049-w
40. Q. Tang, Z. Pan, Z. Ji, H. Chu, H. Pan, D. Li, Oxygen Vacancy-Driven Bandgap Tuning and Ultrafast Laser Performance in Bi2O2Se. SSRN Electron. Journal Jan. (2025). 10.2139/ssrn.5186765
41. A.J. Gayle, Nanostructured Architectures for Solar Thermal and Photocatalytic Applications. Deep Blue (University Michigan) Jan. (2023). 10.7302/7513
42. R.Y. Engel, M. Scholz, J.O. Schunck, M. Beye, A Rate Model of Electron Populations for Non-linear High-Fluence X-ray Absorption Near-Edge Spectra, *arXiv (Cornell University)*, Apr. 2023, 10.3204/pubdb-2023-01186
43. S. Tanvir, S. Pulvin, W.A. Anderson, *MOJ Toxicology*, vol. 1, no. 3, Aug. 2015, 10.15406/mojt.1.3

Figures

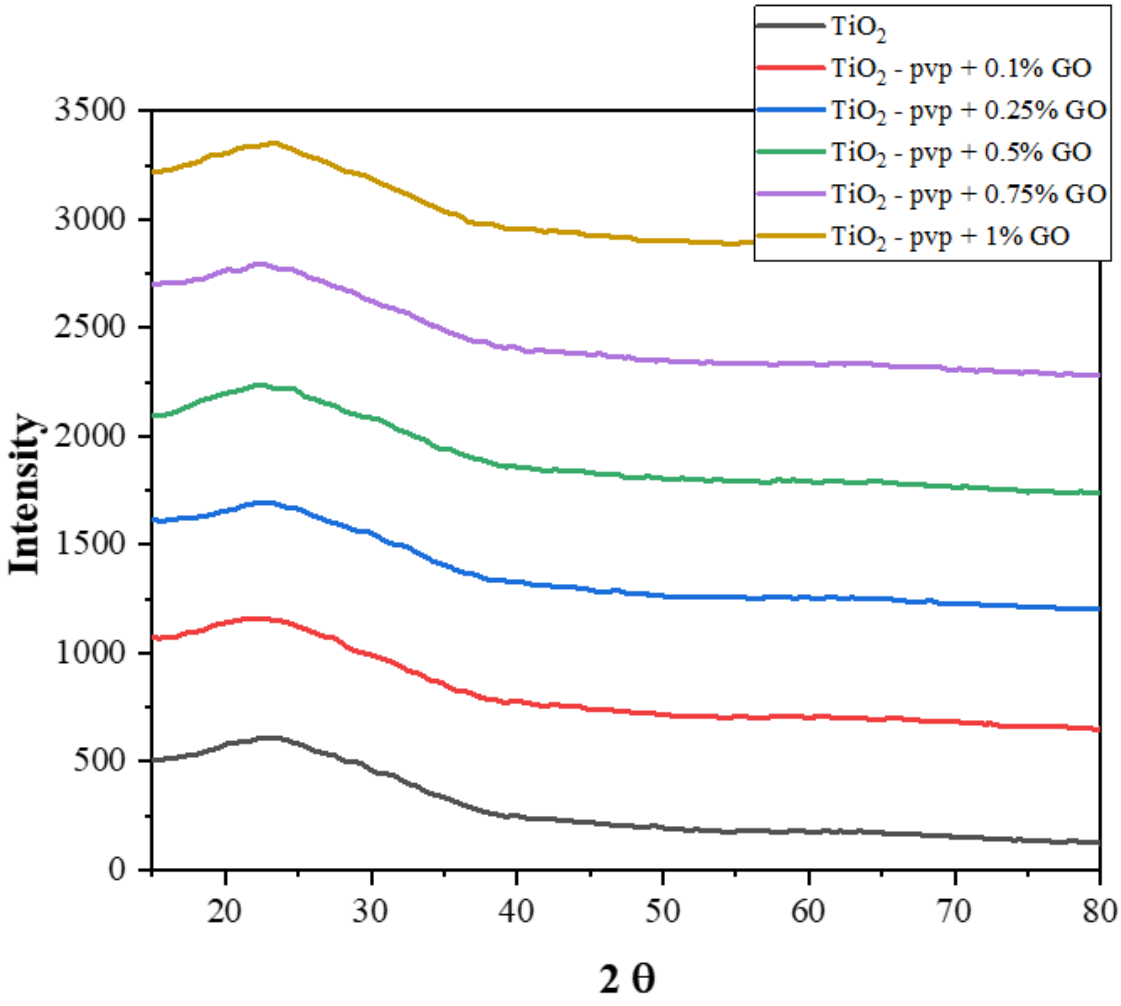


Figure 1

shows the XRD patterns forTiO2 and TiO_2/PVP/GO films with different GO loading.

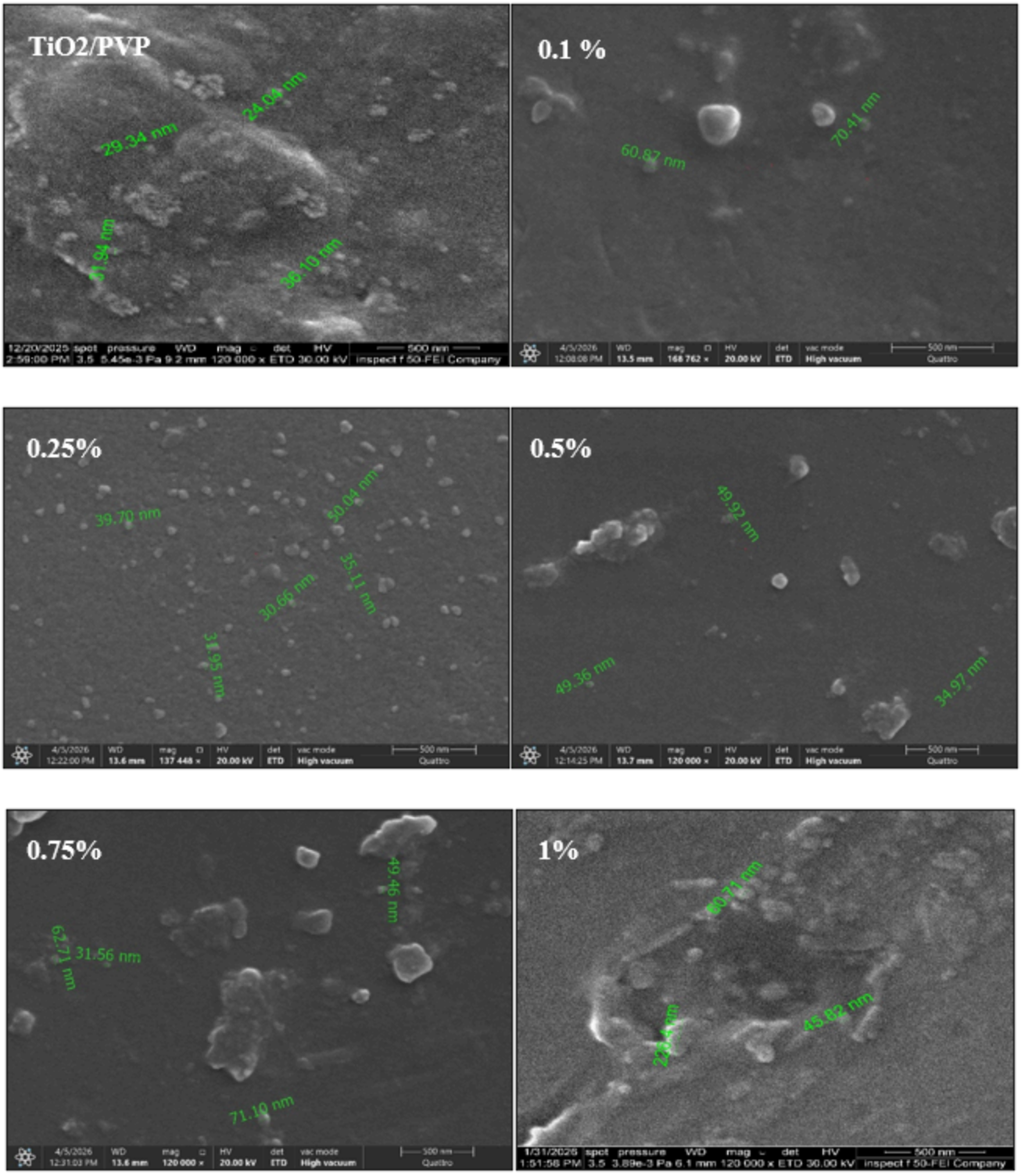


Figure 2

shows the FESEM images forTiO$_2$/PVP and TiO$_2$/PVP/GO films with different GO loading.

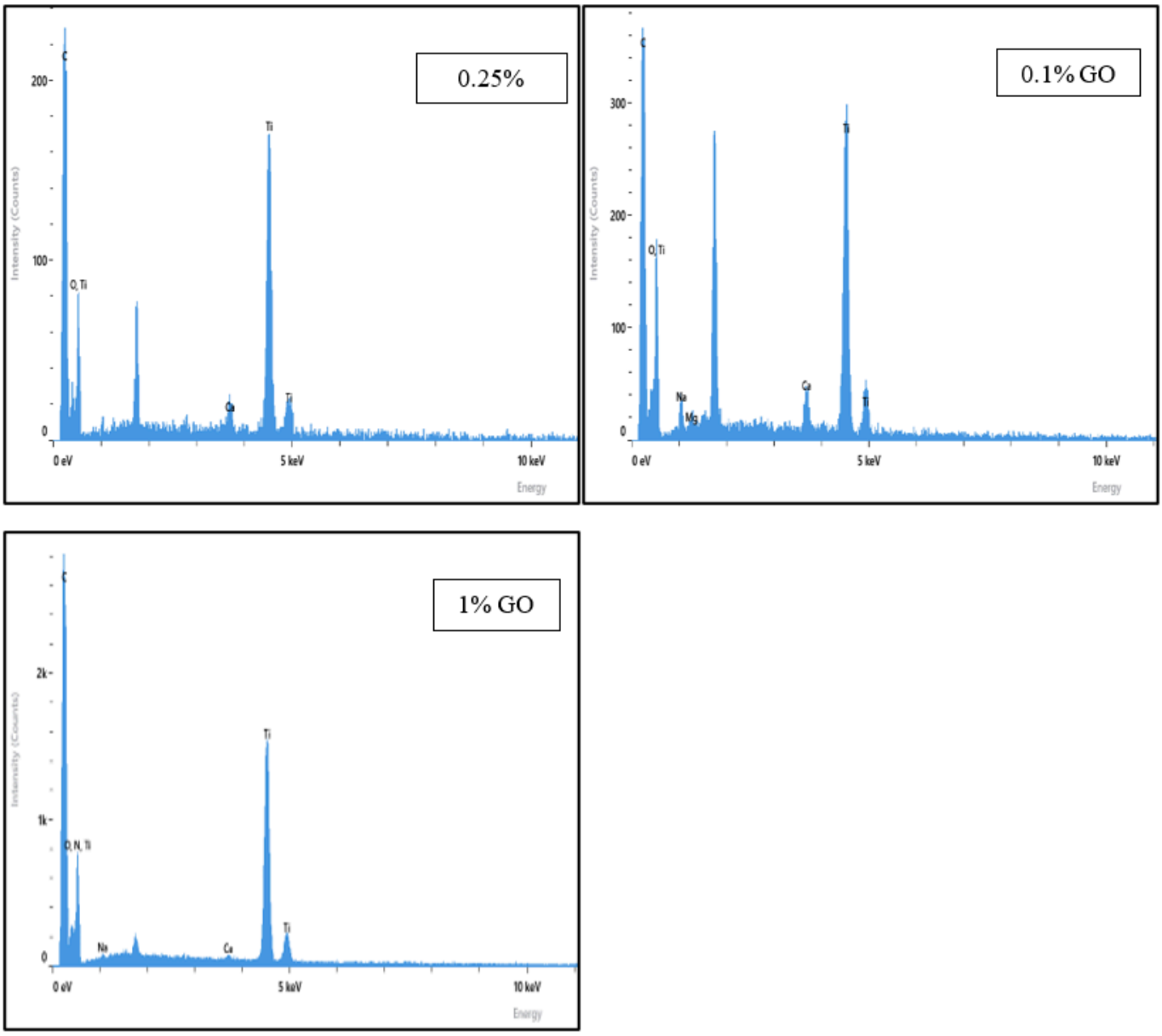


Figure 3

EDS spectra for TiO_2/PVP/GO films with different GO loading.

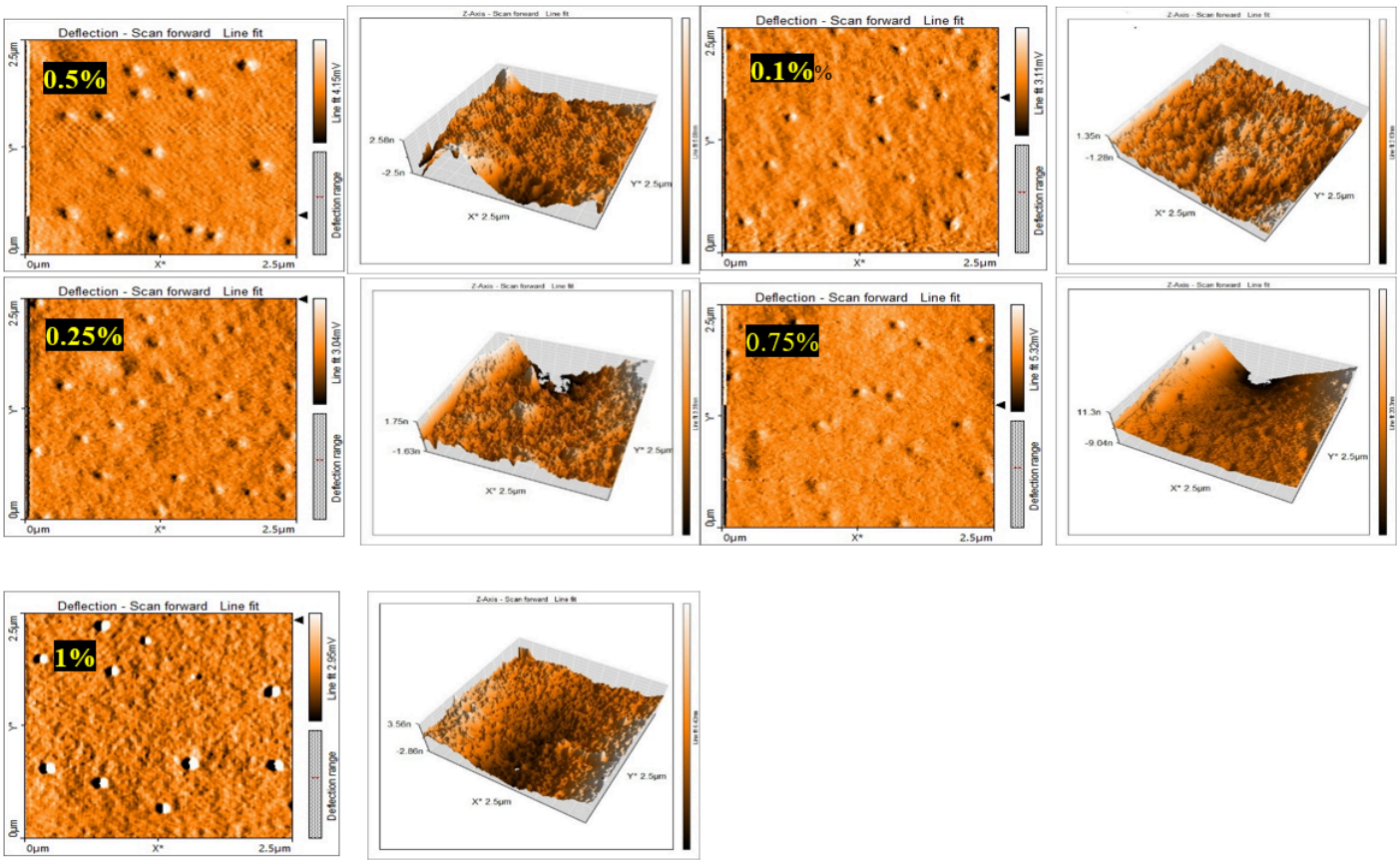


Figure 4

AFM topography Images for TiO_2/PVP/GO films with different GO loading.

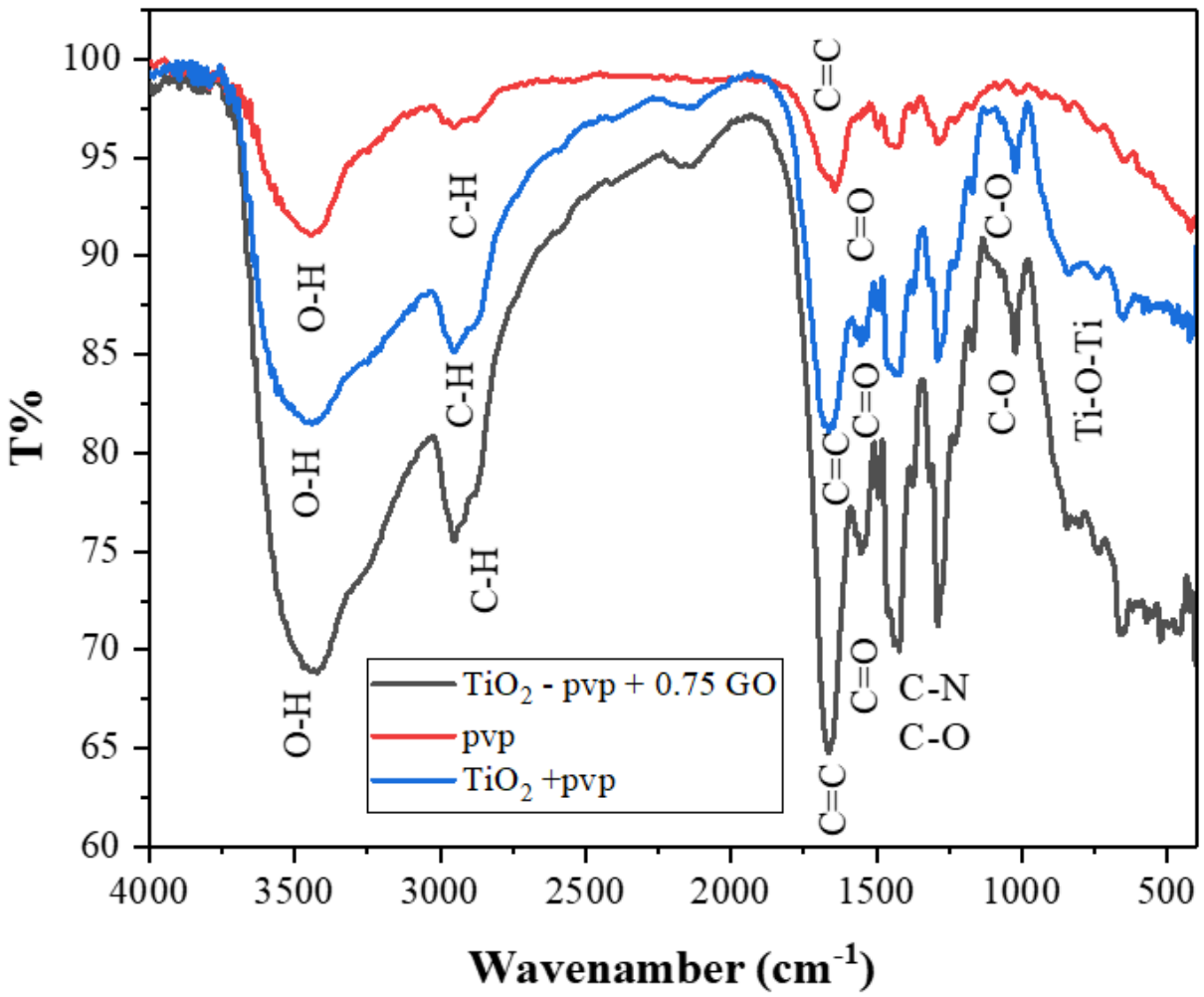


Figure 5

FTIR spectroscopy for TiO_2/PVP/0.7%GO (black line), PVP(red line) and TiO_2/PVP (blue line).

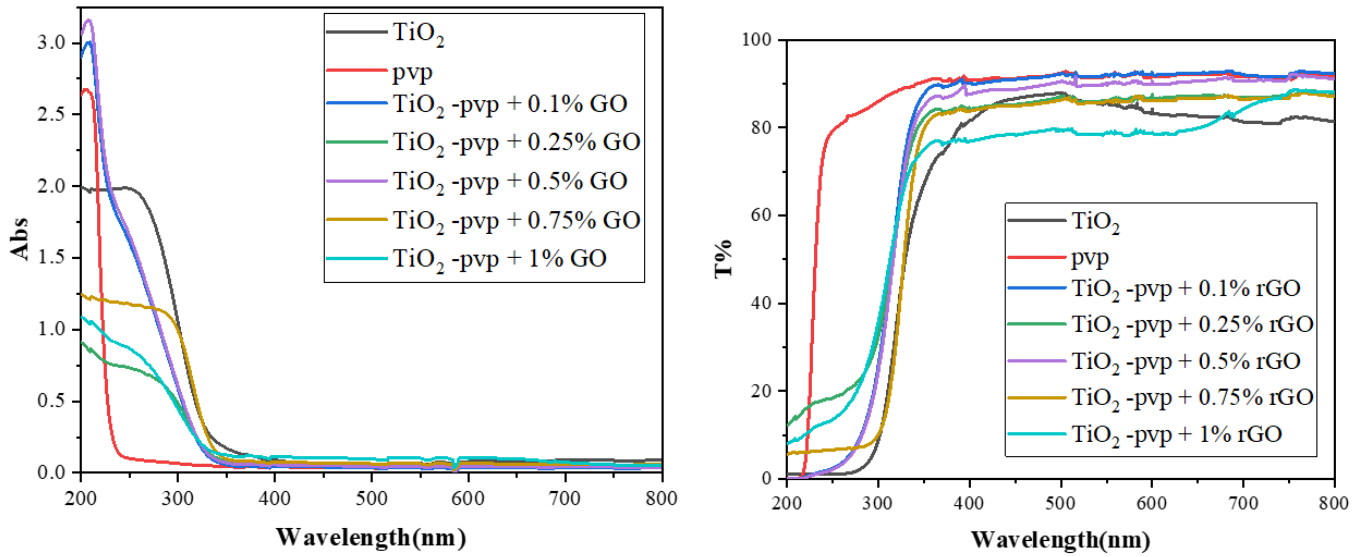


Figure 6

UV–Vis absorbance and transmittance curves forTiO2, PVP and TiO_2/PVP/GO films with different GO loading.

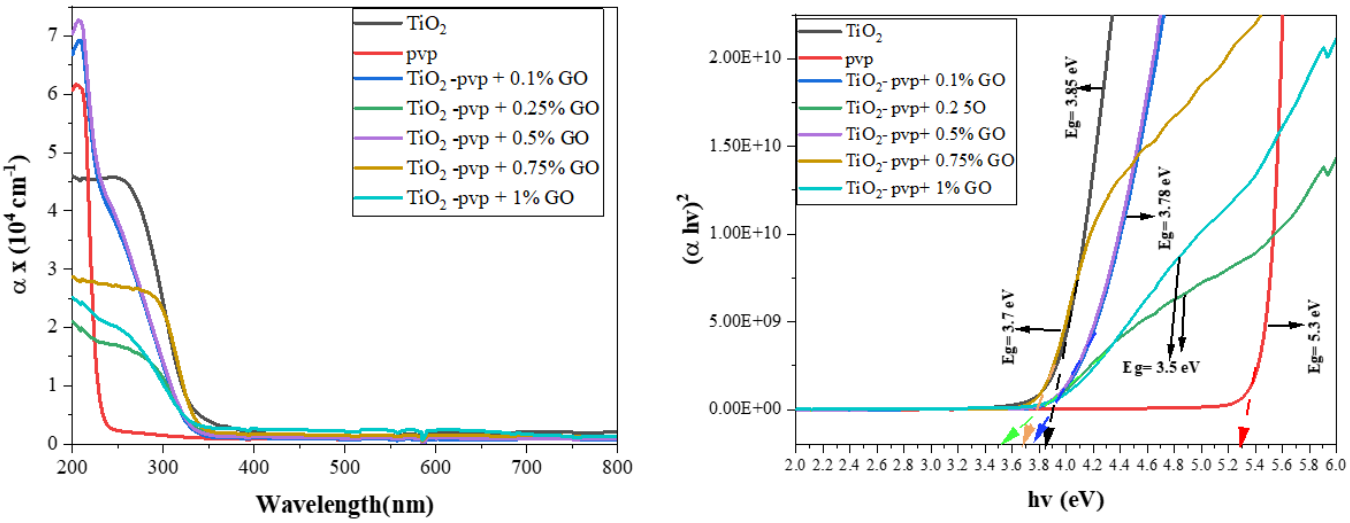


Figure 7

Absorption coefficient and Tauc plot curves forTiO2, PVP and TiO_2/PVP/GO films with different GO loading.